Received March 18, 2020, accepted April 24, 2020, date of publication April 28, 2020, date of current version May 15, 2020.

Digital Object Identifier 10.1109/ACCESS.2020.2990966

Finger Vein Image Inpainting With Gabor Texture Constraints

HANG YANG[1], LEI SHEN[1], YU-DONG YAO[2], (Fellow, IEEE), HUAXIA WANG[3], (Member, IEEE), AND GUODONG ZHAO[4]

[1]College of Communication Engineering, Hangzhou Dianzi University, Hangzhou 310000, China
[2]Stevens Institute of Technology, Hoboken, NJ 07030, USA
[3]College of Engineering, Architecture and Technology (CEAT), Oklahoma State University, Stillwater, OK 74078, USA
[4]Top Glory Tech Limited Company, Hangzhou 310000, China

Corresponding author: Lei Shen (shenlei@hdu.edu.cn)

This work was supported in part by the National Natural Science Foundation of China under Project 61571172, and in part by the Research on blind estimation of multiple PN codes for aperiodic spread spectrum signals.

ABSTRACT The texture edge continuity of a finger vein image is very important for the accuracy of feature extraction. However, the traditional inpainting methods which, without accurate texture constraints, are easy to cause the vein texture of the inpainted image to be blurred and break. A finger vein image inpainting method with Gabor texture constraints is proposed. The proposed method effectively protects the texture edge continuity of the inpainted image. Firstly, using the proposed vertical phase difference coding method, the Gabor texture feature matrix of the finger vein image, which can accurately describe the texture information, can be extracted from the Gabor filtering responses. Then, according to the local texture continuity of the finger vein image, the known pixels, which have different texture orientations with the center pixel in the patch, are filtered out using the Gabor texture constraining mechanism during the inpainting process. The proposed method eliminates irrelevant information interference in the inpainting process and has a more precise texture propagation. Simulation experiments of artificially synthetic images and acquired images show that the finger vein images inpainted by the proposed method have better texture continuity and higher image quality than the traditional methods which do not have accurate texture constraints. The proposed method improves the recognition performance of the finger vein identification system with the acquired damaged images.

INDEX TERMS Finger vein image, Gabor filter, image inpainting, texture feature, vertical phase difference coding.

I. INTRODUCTION

Compared with other biometrics, finger vein [1], [2] has these advantages: non-contact, internal characteristics, living body recognition, high level of security, etc. The recognition performance of a finger vein identification system is very dependent on the image quality [3]. However, due to the multiple scattering interaction in biological tissue, the captured finger vein images are sometimes degraded, resulting in blurring of some vein regions. Reference [4] proposed a bilayer restoration model and [5] proposed a simple and effective scattering removal model, which effectively solve the degradation of finger vein images caused by tissue scattering and improve the visibility of the images. Nonetheless, these methods can be used to restore the degraded image when the image is unpolluted. However, the pollution on the mirror of iacquisition equipment or the peeling finger as shown in Fig. 1 will make a part of the acquired image to be covered, which leads to the loss of image information. The damaged regions will increase the difficulty of finger vein feature extraction and reduce the recognition performance.

FIGURE 1. The conditions which will cause the loss of finger vein image information: polluted equipment mirror and peeling finger.

The associate editor coordinating the review of this manuscript and approving it for publication was Vishal Srivastava.

Therefore, the research on finger vein image inpainting has important theoretical and practical significance. However, the characteristics of finger vein images with different width and extension orientations of vein branches [6] and weak texture edge make that work more difficult.

Many image inpainting methods can be classified into two main categories [7], [8]: structure-based and texture-based. Structure-based inpainting methods [9]–[15] calculate the gradient field or second derivative field of the image and then diffuse information by isophotes from the known regions to the unknown regions point-by-point. Most of the structure-based inpainting methods [9]–[14] are also known as partial differential equations (PDE) based methods or total variational (TV) based methods. These methods ensure local intensity smoothness so that they can inpaint small regions well generally. However, this kind of method essentially ignores the importance of texture information for finger vein images, resulting in blurring when inpainting the vein texture regions. In addition, [15] proposed a fast marching method (FMM). FMM determines the priority by estimating the direction isophotes and then uses the neighborhood pixels for weighting average to fill the damaged region. FMM improves the time efficiency compared to PDE-based methods, but it is blind to use all known information in the patch for weighting calculation, which leads to that the vein texture edge can not be maintained.

Texture-based inpainting [16]–[18] is capable of inpainting larger holes by copying and pasting similar patches in the image using a searching strategy. For example, Criminisi method [16], which combines the advantages of texture synthesis and diffusion filling. However, the priority of the patch is easy to be disordered in the Criminisi method, which leads to the blocky effect in the inpainted image. In recent years, scholars have also proposed many improved methods. Reference [17] improved the Criminisi method by using image structure tensors so that the impact of the image structures is strengthened during the inpainting process. The proposed method tackles two limitations of the image structure propagation and the filling-in order in the image inpainting process. Reference [18] uses a robust priority function to avoid a dropping effect and region segmentation to determine the adaptive patch size and reduced search region.

Recently, there have been some inpainting methods, which combine structure and texture information [19]–[21]. Bertalmio *et al.* [20] proposed an inpainting method combining texture synthesis and PDE. In this method, the image is decomposed into texture and structure components. Then reconstruct each of them separately with structure and texture filling-in algorithms to complete the inpainting task. Reference [21] proposed a PDE-based image inpainting method using an anisotropic heat transfer model, which can simultaneously propagate the structure and texture information. Although this kind of method combines the advantages of the two, it increases the complexity of the method and has limited ability to improve the performance in finger vein image inpainting.

The Criminisi method and those described above improved methods select the best matching patch by the sum of square difference (SSD) distance criterion or other grayscale information of the patch, which can not accurately describe the texture of finger vein images. It may lead to matching errors and image information loss when inpainting the vein texture regions of the finger vein image.

Recently, with the rapid development of deep learning, it has achieved good results in such fields as finger vein image process and recognition. Reference [22] proposed a convolutional neural network (CNN) to train and restore the vein patterns, which tackles the problem of vein pattern loss caused by overexposure or blurred region in the finger vein images. Reference [23] proposed a new model based on the pulse coupled neural network (PCNN) to enhance finger vein image quality and further to improve the reliability of image recognition. Reference [24] applied CNN to finger vein recognition and achieved better performance than traditional algorithms. However, their research topics are based on the unpolluted finger vein images. There is a lack of deep learning research on the inpainting methods of the damaged finger vein images.

In this paper, a finger vein image inpainting method with Gabor texture constraints is proposed to tackle the texture edge discontinuity of the inpainted finger vein image. First, the Gabor texture feature matrix (GTFM) of the finger vein image is extracted from Gabor filter responses using a proposed vertical phase difference coding method. The GTFM can accurately describe the texture information of the finger vein image. Then, the known pixels, which have different texture orientations with the center pixel in the patch, will be filtered out by the Gabor texture constraining mechanism during the inpainting process. The Gabor texture constraining mechanism makes the proposed method has a more precise texture propagation. The vein texture of the inpainted finger vein image is more complete and coherent than the traditional inpainting methods which do not have accurate texture constraints.

The rest of the paper is organized as follows. Section II presents a vertical phase difference coding method based on Gabor filter. Section III presents a finger vein image inpainting method given Gabor texture constraints. The experimental results and analysis are given in Section IV. Section V gives a summary of the paper.

II. VERTICAL PHASE DIFFERENCE CODING METHOD BASED ON GABOR FILTER

Two-dimensional Gabor filter is very sensitive to the texture edge of the image and its expression of frequency and orientation is consistent with the texture recognition mechanism of the human vision system [25]. Gabor filter can effectively enhance the edge, peak, valley, ridge contours and other underlying feature information. Moreover, the Gabor filter has good scale characteristic and directivity, which can match the characteristics of finger vein images, such as different width and extension orientation of vein branches. And the

Gaussian kernel component of the Gabor filter can be robust to noise interference. So compared to the gradient operator which can be greatly disturbed by light intensity and noises, Gabor filter can extract texture edge of finger vein images more stably and accurately.

A. EXTRACT TEXTURE EDGE BY GABOR FILTER BANK

The Gabor filter is a Gaussian function windowed by a sine plane wave, which is expressed as follows [26], [27]:

$$g(x, y; \lambda, \theta, \psi, \sigma, \gamma) = e^{-\frac{x'^2+\gamma^2 y'^2}{2\sigma^2}} \cdot e^{i(2\pi \frac{x'}{\lambda}+\psi)} \tag{1}$$

where $x' = x\cos\theta + y\sin\theta$, $y' = -x\sin\theta + y\cos\theta$; λ and ψ are the wavelength and the phase offset of sine wave function, respectively; σ is Gaussian standard deviation, also known as the spatial scale factor; γ is the spatial aspect ratio of the Gabor filter. The parameters are related to the size of images used in this paper, 200×84. Thus, set $\lambda = 17$, $\psi = 0$, $\gamma = 1$, and the three scales are $\sigma_1 = 3$, $\sigma_2 = 3.4$, $\sigma_3 = 3.8$. θ is orientation parameter that determines the directivity of Gabor filter, which can be expressed as follows:

$$\theta_k = (k-1)\frac{\pi}{N}, \quad \theta_k \in [0\ ,\ \pi), \quad k \in [1, N] \tag{2}$$

where N is the total number of orientations. According to the characteristics of vein structure, we set $N = 8$ after a lot of experiments. θ_k represents the k^{th} orientation, π/N is the angular interval.

The real component g_{re} and the imaginary component g_{im} of the Gabor filter can be obtained by decomposing the sine wave part of Eq. 1:

$$g_{re}(x, y; \lambda, \theta, \psi, \sigma, \gamma) = e^{-\frac{x'^2+\gamma^2 y'^2}{2\sigma^2}} \cdot \cos(2\pi \frac{x'}{\lambda} + \psi) \tag{3}$$

$$g_{im}(x, y; \lambda, \theta, \psi, \sigma, \gamma) = e^{-\frac{x'^2+\gamma^2 y'^2}{2\sigma^2}} \cdot \sin(2\pi \frac{x'}{\lambda} + \psi) \tag{4}$$

After convoluting them with the original finger vein image $F(x, y)$, the coefficient amplitude can be obtained by taking the modulo according to

$$H_{k,\sigma}(x, y) = \sqrt{H_{k,\sigma}(x, y)_{re}{}^2 + H_{k,\sigma}(x, y)_{im}{}^2} \tag{5}$$

where $H_{k,\sigma}(x, y)_{re} = F(x, y) * g_{re}(x, y; \theta_k, \sigma)$, $H_{k,\sigma}(x, y)_{im} = F(x, y) * g_{im}(x, y; \theta_k, \sigma)$, are the filter responses of the real component and the imaginary component at k^{th} orientation and σ scale respectively. $H_{k,\sigma}(x, y)$ is the coefficient amplitude, which represents the energy of images in that orientations and scales as shown in Fig. 2.

The larger the coefficient amplitude is, the richer the texture edge information is saved on that scale. Thus, firstly, we select the largest of the three scales as the amplitude coefficient of each point in that orientation:

$$H_k(x, y) = \max(H_{k,\sigma_i}(x, y)), \qquad i = 1, 2, 3 \tag{6}$$

The responses $H_k(k = 1, 2, \ldots, 8)$ in 8 orientations are obtained by using Eq. 6.

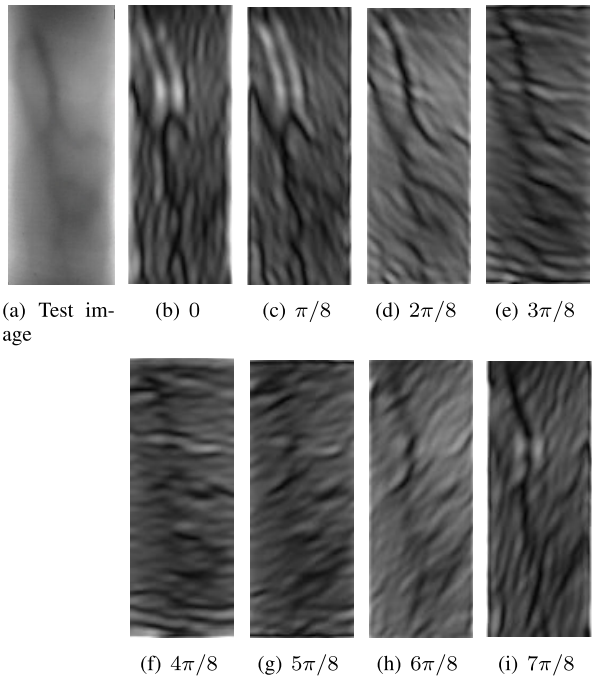

(a) Test image (b) 0 (c) $\pi/8$ (d) $2\pi/8$ (e) $3\pi/8$ (f) $4\pi/8$ (g) $5\pi/8$ (h) $6\pi/8$ (i) $7\pi/8$

FIGURE 2. Test image and the Gabor filtering responses in different orientation θ ($\sigma = 3.4$).

B. VERTICAL PHASE DIFFERENCE CODING METHOD

According to the principle that the texture edge information difference between the two orientations along the finger vein and vertical to the finger vein is the largest, a vertical phase difference coding method is proposed in this paper. The filtering responses H_k in 8 orientations are divided into 4 groups (H_1 and H_5, H_2 and H_6, H_3 and H_7, H_4 and H_8) according to the mutual vertical orientation. After calculating the absolute value of the difference of each group, the group with the largest result will be picked as follows

$$\Delta H_{k_{\max}} = \max(\left|H_k - H_{k^\perp}\right|), \quad k^\perp = k + 4 \tag{7}$$

where $k \in [1, 4]$, the orientations $k_{\max}$ and ${k_{\max}}^\perp$ of the group $\Delta H_{k_{\max}}$ are the possible texture orientations of the pixel to be repaired. The larger the response amplitude is, the stronger the texture edge information energy is in that orientation. Therefore, the Gabor texture feature matrix of the finger vein image can be finally obtained by using the following equation

$$\text{GTFM}(x, y) = \begin{cases} k_{\max}, & H_{k_{\max}}(x, y) > H_{{k_{\max}}^\perp}(x, y) \\ {k_{\max}}^\perp, & else \end{cases} \tag{8}$$

where $H_{k_{\max}}$ and $H_{{k_{\max}}^\perp}$ are the Gabor filtering responses at the $k_{\max}$ direction and the ${k_{\max}}^\perp$ direction respectively.

Fig. 3 shows the test image and the corresponding GTFM. Combining Fig. 3(a) and Fig. 3(b) shows that the GTFM of finger vein image clearly indicates the texture trend of the vein regions and the background regions, including some texture edge of slight veins. In addition, the texture feature distribution of the image blocks located on the same vein structure has a high degree of similarity. These characteristics demonstrate that GTFM accurately describes the texture

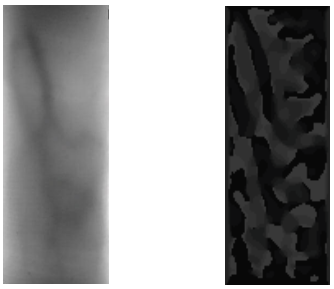

(a) (b)

FIGURE 3. (a) Test image; (b) The GTFM extracted from (a).

information of the finger vein image. Thus GTFM can be used for auxiliary correction to protect the vein texture edge of the finger vein image during the inpainting process.

As for the damaged finger vein images, the convolution window on the contour of the damaged border contains unknown pixels. The grayscale values of the unknown pixels in the window are set to zero so that those pixels do not affect the accuracy of convolution calculation. Finally, the known pixels are encoded and assigned texture feature values, while the texture feature value of the unknown pixels (damaged pixels) is set to zero, according to

$$\mathrm{GTFM}(x,y)=\begin{cases} k_{\max}, & H_{k_{\max}}(x,y) > H_{k_{\max}{}^{\perp}}(x,y), \\ & \text{is known} \\ k_{\max}{}^{\perp}, & H_{k_{\max}}(x,y) <= H_{k_{\max}{}^{\perp}}(x,y), \\ & F(x,y) \text{ is known} \\ 0, & F(x,y) \text{ is unknown} \end{cases} \quad (9)$$

III. IMAGE INPAINTING WITH GABOR TEXTURE CONSTRAINTS

As for the traditional methods which do not have accurate texture constraints, due to mixing low texture correlation information in the filling calculation, the vein texture of the inpainted image will be discontinuous. The proposed method utilizes GTFM to constrain the texture propagation in the inpainting process. The specific steps of the proposed method are as follows.

A. DETERMINATION OF PRIORITY

Priority is an important factor affecting the performance of image inpainting methods. Sethian [28] proposed fast-marching level-set methods to track the moving edge, which can simulate the curve evolution process of the contour of a damaged region. It starts from the contour and gradually spreads to the interior, point by point, until all unknown pixels are filled. It ensures that the filling sequence is more in line with the human visual psychology. The time of the contour passes through each pixel can be expressed as $T(i,j)$ and the priority of the proposed inpainting method can be determined by $T(i,j)$. The pixels with the smallest $T(i,j)$ value will be filled first. The diffusion of the contour satisfies the conditions of the Eikonal equation [28]:

$$|\nabla T| = 1/v_{i,j} \quad (10)$$

where $v_{i,j}$ is the diffusion speed of the contour of the damaged region and $v_{i,j} = 1$ means moving one pixel at a time.

Using the inverse difference method to solve Eq. 10, we can get $T(i,j)$ of each unknown pixel:

$$\left\{\begin{bmatrix} \max\left(D_{i,j}^{-x}T, D_{i,j}^{+x}T, 0\right)^2 + \\ \max\left(D_{i,j}^{-y}T, D_{i,j}^{+y}T, 0\right)^2 \end{bmatrix}\right\}^{\frac{1}{2}} = 1 \quad (11)$$

where $D_{i,j}^{-x}T, D_{i,j}^{+x}T, D_{i,j}^{-y}T, D_{i,j}^{+y}T$ are the forward and backward differences of the time function T in the horizontal x orientation and the vertical y orientation respectively. The detailed calculation process can be found in [28].

B. DETERMINATION AND UPDATE OF THE MAIN TEXTURE ORIENTATION

Fig. 4(b) and Fig. 4(c) show the Gabor texture feature information in the patch centered on damaged pixels A and B, respectively. The pixel A is located in the vein region, while the pixel B is located in the background region. The feature values of the unknown pixels are zero and other non-zero values are the known pixels. Combining the observations in Fig. 4(a) to 4(c) shows again that the texture trends of the vein regions or the background regions in the local image are continuous. Those pixels with the same texture trend have the same texture feature value. Therefore, we select the mode

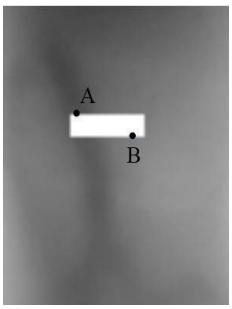

(a)

1	2	2	2	3	5	5
1	2	2	2	2	3	5
1	2	2	2	2	3	5
1	0	0	0	0	0	0
1	0	0	0	0	0	0
1	0	0	0	0	0	0
1	0	0	0	0	0	0

(b)

0	0	0	0	0	0	0
0	0	0	0	0	0	0
0	0	0	0	0	0	0
0	0	0	0	0	0	0
6	7	7	7	7	7	7
6	7	7	7	7	7	6
6	7	7	7	7	7	6

(c)

FIGURE 4. (a) Damaged pixels A and B; (b) The Gabor texture features of the patch centered on pixel A, located in the vein region; (c) The Gabor texture features in the patch centered on pixel B, located in the background region.

of the Gabor texture feature value of all known pixels in the patching window as the main texture feature of that window.

As shown in Fig. 5, $B_\varepsilon(p)$ is the patch centered on pixel p and its diameter is ε. The known regions and the unknown regions can be determined by the mask binary image, in which the value of pixels in the known region is 1, while that in the unknown region is 0. And the mask binary image can be obtained by the fuzzy c-means (FCM) segmentation algorithm [29]. GTFM $_{B_\varepsilon(p)|\text{ known}}$ represents the Gabor texture feature of all known pixels in $B_\varepsilon(p)$. Then the texture feature value of p is updated as follows:

$$mto_{B_\varepsilon(p)} = \text{Mode}(\text{GTFM}_{B_\varepsilon(p)|\text{ known}}) \tag{12}$$

$$\text{GTFM}(p) = mto_{B_\varepsilon(p)} \tag{13}$$

where $mto_{B_\varepsilon(p)}$ is the main texture orientation of $B_\varepsilon(p)$. Too small a patch may lead to too little known pixels being available during the inpainting, and too large a patch may introduce too much noise, affecting the determination of the main texture orientation. The size of the patch is set to 7×7 after a lot of experiments. As a result, the texture feature of damaged pixels A and B in Fig. 4(a) will be updated to 2 and 7 after filling, respectively. It is in line with the texture trend of the finger vein image.

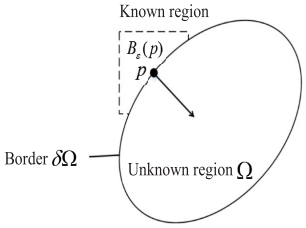

FIGURE 5. Schematic of patch $B_\varepsilon(p)$.

C. GABOR TEXTURE CONSTRAINING MECHANISM AND WEIGHT COEFFICIENT OF INPAINTING

Considering that texture continuity is very important for the inpainted finger vein image, the proposed method gives the priority to the texture correlation between the pixels during inpainting. Firstly, according to the main texture direction obtained in Eq.12, the proposed method uses the Gabor texture constraining mechanism to eliminate the interference of information with different texture orientations in the filling calculation. The Gabor texture constraining mechanism enables the proposed method achieve a more precise texture propagation. Secondly, according to the grayscale and distance correlation between the pixels, the proposed method inpaints the damaged finger vein image by weighting the remaining known pixels which are in the same texture direction.

In Fig. 5, the pixels in the dotted box part outside Ω are known. Those known pixels will be used to fill the unknown pixel p. Before this, the known pixels that have different texture orientations with the center point will be filtered out by the Gabor texture constraining mechanism as shown in Fig. 6.

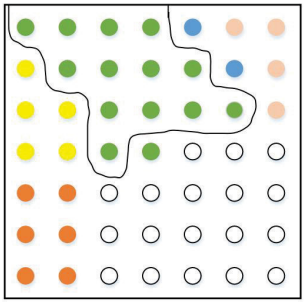

FIGURE 6. Schematic of the Gabor texture constraining mechanism.

Fig. 6 shows the distribution of the Gabor texture features in the patch and different colors represent different texture direction features. The white points and the center point of the patch are the damaged pixels whose information is unknown and the other color points (except the center point) are known. The texture feature value of the center point has been assigned by the main texture orientation of that patch. The green points and the center point are located on the same vein texture trend and have the same texture orientation, while the other non-green points have different texture orientations with the center point. The proposed method will filter out the points with different texture orientations and select the green points for weighting calculations. The Gabor texture constraining mechanism makes the inpainting process free from the 'noises' with low texture correlation, which plays a role in maintaining the vein texture edges and avoiding blurring the inpainted region.

Fig. 7(a) to 7(c) are the GTFM extracted from the original image, the damaged image (obtained by manually adding a damaged region to the original image), and the inpainted image (obtained by inpainting the damaged image by the proposed method) respectively. It can be seen that the GTFM of the inpainted image restores the vein texture trend of the original image, which demonstrates that the Gabor texture constraining mechanism can constrain the inpainting process accurately following the texture trend.

FIGURE 7. (a) The GTFM extracted from the original image; (b) The GTFM extracted from the damaged image; (c) The GTFM extracted from the inpainted image.

i At the same time, considering the spatial and the grayscale correlation between the pixels of the finger vein image,

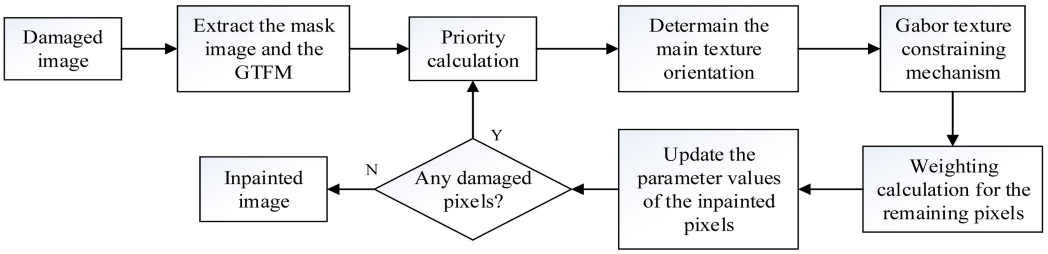

FIGURE 8. The flowchart of the proposed method.

the proposed method sets the distance factor and the gray factor to weight the remaining known pixels as follows:

1) Firstly, calculate the average grayscale avg of the remaining known pixels. Then the absolute values of the difference between q and avg, and the Euclidean distance between q and the center pixel p can be calculated as follows

$$\text{avg} = \text{Mean}(F(q)), q \in \{x \,|\text{GTFM}(x) = \text{GTFM}(p)\} \tag{14}$$

$$\text{gray}(p, q) = |F(q) - \text{avg}| \tag{15}$$

$$\text{dst}(p, q) = \|p - q\|^2 \tag{16}$$

where $x \in B_\varepsilon(p)|_{\text{known}}$, q is one of the remaining known pixels. gray is the gray factor. The pixels whose grayscale value is closer to avg get greater weight. dst is the distance factor. The pixels which are closer to the center pixel p get greater weight.

2) The weight of each remaining known pixel q is obtained by using the exponential component of the standard normal distribution model:

$$w(p, q) = \exp(-\frac{(\text{gray}(p, q) \cdot \text{dst}(p, q))^2}{2}) \tag{17}$$

3) Weights normalization:

$$W(p, q) = \frac{w(p, q)}{\text{sum}(w)} \tag{18}$$

4) The final weighting equation is defined as follows:

$$\hat{F}(p) = \sum\nolimits_{x \in B_\varepsilon(p)|_{\text{known}}} W(p, q) \cdot F(q), \quad q \in \{x \,|\text{GTFM}(x) = \text{GTFM}(p)\} \tag{19}$$

where $\hat{F}(p)$ is the value of pixel p after inpainting.

D. THE OVERALL FLOW OF PROPOSED METHOD

Fig. 8 shows the flowchart of the proposed method and the specific steps are as follows:

(1) Firstly, the proposed method uses the fuzzy c-means (FCM) segmentation algorithm [29] to get the mask binary image and then extract the GTFM of the finger vein image by the vertical phase difference coding method proposed in Section II.

(2) Using a fast-marching level-set method, the time value of the damaged pixels on the contour of the damaged region can be obtained to determine the priority.

(3) The main texture orientation of the patch can be determined by GTFM. Then the method uses the Gabor texture constraining mechanism to filter out the known pixels, which have different texture orientations from the main texture orientation in the patch.

(4) The remaining known pixels are used for weighting calculation to fill the damaged pixel. Then the time value and the Gabor texture feature of the inpainted pixel will be updated.

(5) Repeat Steps (2), (3) and (4) until finish inpainting.

IV. EXPERIMENT RESULTS AND EVALUATION

The proposed method is compared with three traditional inpainting methods by experiments on the artificially synthetic finger vein images and the acquired finger vein images, respectively. The iteration times of the method based on TV model [9] are set to 1000. The patch size of the Crinimisi method [16] and the FMM method [15] are the same as that of the proposed method, which is set to 7×7. Besides the subjective evaluation of the human visual system, mean square error (MSE) and peak signal to noise ratio (PSNR) are used to evaluate the inpainting quality of the artificially synthetic damaged images. False rejection rate (FRR) and false acceptance rate (FAR) are also used to evaluate the inpainting quality of the acquired damaged images.

A. ARTIFICIALLY SYNTHETIC DAMAGED IMAGE

As shown in Fig. 9, the artificially synthetic damaged image Fig. 9(b) was obtained by adding four damaged regions to the test image Fig. 9(a). The location of each region is different:

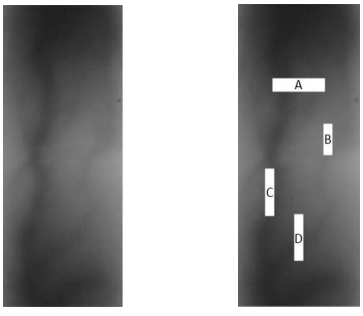

(a) (b)

FIGURE 9. (a) Test image; (b) Artificially synthetic damaged image obtained by (a).

A horizontally covers a wider vein; B is located in a smooth background region; C covers a vein vertically; D covers a slight vein with blurred texture. The types of damaged images in practical applications are mostly included in these cases.

1) SUBJECTIVE EVALUATION AND ANALYSIS

Fig. 10(a) to 10(d) show the results of three traditional inpainting methods and the proposed method and the inpainted regions are enhanced for the convenience of observation.

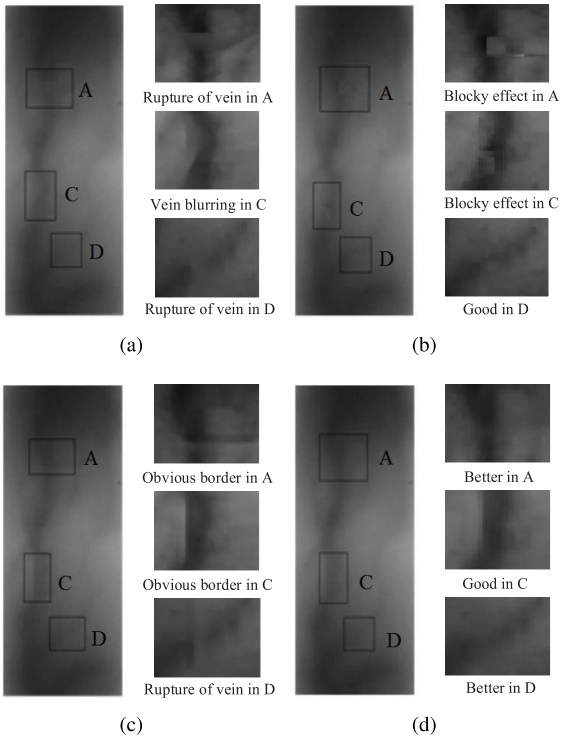

FIGURE 10. Comparison of inpainting using different methods. (a) Method based on TV model; (b) Crinimisi method; (c) FMM method; (d) The Proposed method.

It can be seen that for the damaged region A and C, where the veins are masked, the vein texture of the result Fig. 10(a) inpainted by the method based on TV model is blurred and incoherent and the vein is cut off visually; The result Fig. 10(b) inpainted by the Crinimisi method has an obvious blocky effect, which affects the edge of a vein; In the result Fig. 10(c) of the FMM method, the vein edge was blurred or the boundary of the inpainted region was obvious, and the effect of edge retention is unsatisfactory. For the damaged region B located in the smooth background region, all these methods work well. As for the damaged region D with low contrast, the vein structure in this region is slight and blurred. The method based on TV model or FMM caused blur and rupture to the vein structure, while the Crinimisi method and the proposed method do better in inpainting slight veins. As shown in Fig. 10(d), due to the Gabor texture constraining mechanism, the proposed method has a precise texture propagation and the image inpainted by the proposed method has a better effect on vein edge retention and visual connectivity.

2) OBJECTIVE EVALUATION AND ANALYSIS

The comparison of the performance parameters in Table 1 shows that the proposed method has higher image quality than the other three traditional methods without accurate texture constraints.

TABLE 1. Image quality evaluation comparison inpainted by different methods.

Methods	MSE	PSNR/dB
Method based on TV model	0.2643	53.9104
Crinimisi method	0.5004	51.1380
FMM method	0.1561	56.1976
The proposed method	0.1229	57.2368

B. ACQUIRED DAMAGED IMAGE

The above experiments have demonstrated the effectiveness of the proposed method for the artificially synthetic damaged images. The research in this part will be performed on the acquired damaged images. Because of the vein images in the current public databases are all acquired under normal conditions, such special case images are lacking. Thus, the databases used in this part consist of the images acquired under damaged conditions and the same users under normal conditions, by a laboratory at Hangzhou Dianzi University (HDU).

The damaged image includes two conditions: the mirror of the acquisition equipment is polluted or the fingers are peeling. A total of 40 fingers of 20 volunteers (15 men and 5 women), whose fingers have peeled, were acquired. Under normal condition and two kinds of damage conditions, 10 images are collected for each finger respectively, $40 \times 10 \times 3 = 1200$ in total. These acquired images constitute a normal finger vein image database named NFVI and two damaged finger vein image databases named DFVI. Then, the NFVI and two other DFVIs are respectively composed into two mixed finger vein image databases named MFVI, each finger class in MFVI contains 10 normal images and 10 damaged images. For the acquired damaged images, the original images cannot be obtained, so it is no longer meaningful to use MSE and PSNR for evaluation. Therefore, the FRR and FAR of intra-class and inter-class samples are used to verify the effectiveness of inpainting methods. After the damaged images in the MFVIs being inpainted by different inpainting methods, all of the images in the MFVIs will be processed by the guide filter enhancement method [30], the Niblack [31] segmentation method, and the Zhang-Suen thining method [32] to obtain the finger vein skeleton features. Finally, the modified Hausdorff distance (MHD) [33] method is used for recognition and each MFVI can obtain 7,600 intra-class matching data and 312,000 inter-class matching data. The recognition performance comparison is shown in Table 2.

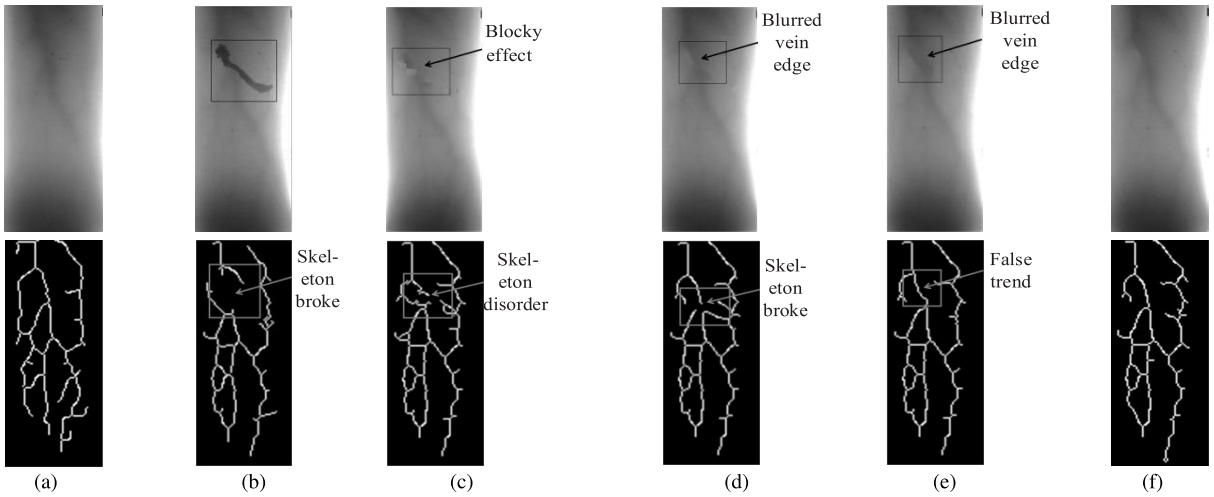

FIGURE 11. Inpainting comparison of different methods on the image of peeling finger, and the skeletons extracted from corresponding images. (a) Normal image; (b) Damaged image; (c) Crinimisi method; (d) FMM method; (e) Method based on TV model; (f) The proposed method.

TABLE 2. FRR(%) comparison when FAR is 0 after being inpainted by different method.

Methods	MFVI	
	Polluted Equipment mirror	Peeling finger
Without any method	28.91	31.51
Method based on TV model	23.54	24.39
FMM method	23.10	27.43
Crinimisi method	22.12	28.61
The proposed method	20.12	23.25

1) MFVI WITH IMAGES OF PEELING FINGERS

It can be seen from Fig. 11(b) that, when the user's finger is peeling, there will be a slender strip-shaped damaged region in the acquired image. The damaged region is similar to the vein structure in grayscale and covers a part of the vein structure, which causes the vein structure in this region to break in the skeleton. In the result Fig. 11(c) inpainted by the Crinimisi method, the blocky effect existing in the inpainted region can be clearly seen and that region in the corresponding skeleton is also disordered. From the result Fig. 11(d) of the FMM method, the vein edge becomes blurred after being inpainted, which causes the vein of that region in the skeleton to break. From the result Fig. 11(e) inpainted by the method based on the TV model, it can be seen that the connection of the vein structure is incoherent, causing a false skeleton trend in that region. While inpainted by the proposed method, both the result and the skeleton in Fig. 11(f) are more in line with the vein texture structure of the image acquired under normal conditions.

The receiver operating characteristic (ROC) curve [34] in Fig. 12 shows that such a peeling region seriously affects the grayscale distribution of the image, which leads to inaccurate segmentation and reduces the recognition performance. Combined with Table 2, it can be seen that, when the FAR is 0, the FRR of the proposed method is 23.25%, TV model is 24.39%, FMM method is 27.43%, Crinimisi method is 28.6%, while without any inpainting method is 31.51%, respectively. It shows the best recognition performance after being inpainted by the proposed method.

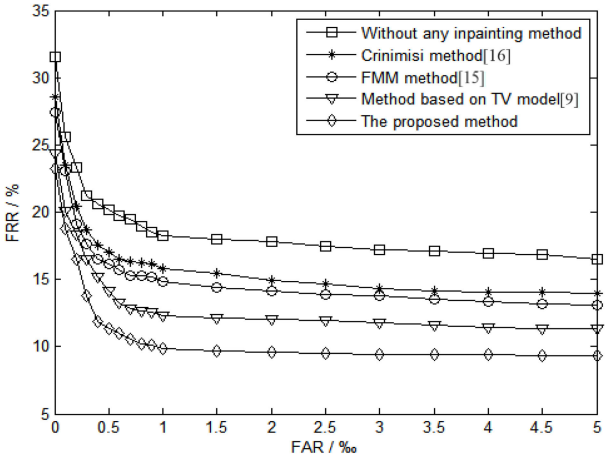

FIGURE 12. Recognition performance of MFVI with images of peeling fingers, after being inpainted by different methods.

2) MFVI WITH IMAGES OF POLLUTED EQUIPMENT MIRROR

Fig. 13(b) shows another type of damaged image in practical applications. When there is a dirty block on the mirror of the acquisition equipment, a black block region will appear on the acquired image, resulting in the loss of image information in this region. Although the black block has been removed in the result Fig. 13(c) of the method based on TV model, the visual continuity is poor and the skeleton is not consistent with the original vein trend. In the result Fig. 13(d) of the FMM method, there are certain obvious repair boundaries in that region, which leads to the false trend of the vein skeleton. In the result Fig. 13(e) of the Crinimisi method, the edges of the veins are blurred, resulting in a false skeleton. The

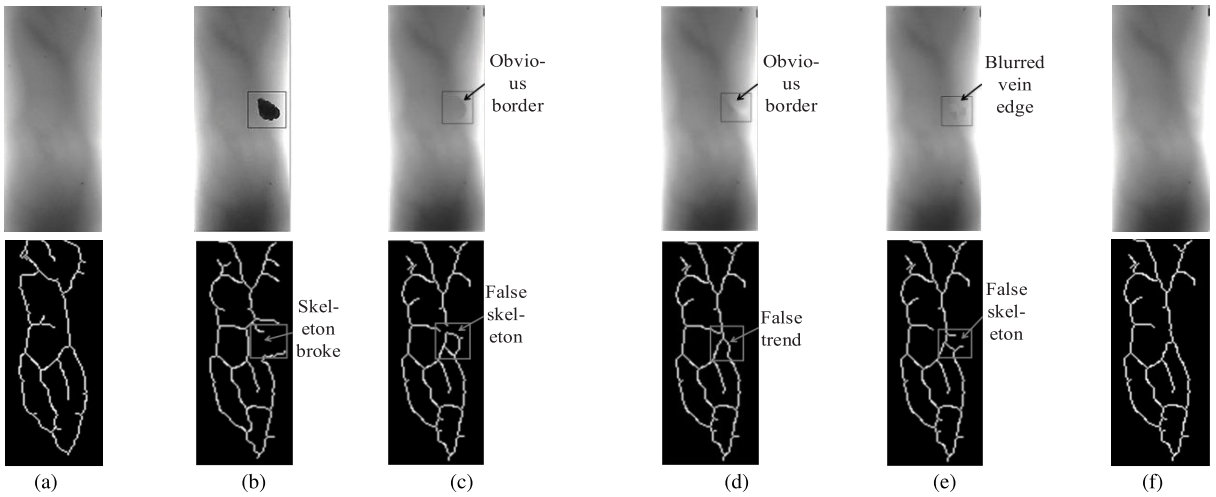

FIGURE 13. Inpainting comparison of different methods on the image of polluted equipment mirror, and the skeletons extracted from corresponding images. (a) Normal image; (b) Damaged image; (c) Method based on TV model; (d) FMM method; (e) Crinimisi method; (f) The proposed method.

proposed method uses the GTFM to constrain texture propagation, which maintains the texture edges of the inpainted result Fig. 13(f) better, so that the skeleton maintains the same vein structure as the image acquired under normal conditions.

The ROC curve in Fig. 14 shows that, if such a block damaged region exists in the finger vein image, the original vein structure will be masked and the recognition performance will be reduced. Combined with Table 2, it can be seen that, when the FAR is 0, the FRR of the proposed method is 20.12%, Crinimisi method is 22.12%, FMM method is 23.10%, TV model is 23.54%, while without any inpainting method is 28.91%, respectively. It shows the best recognition performance after being inpainted by the proposed method.

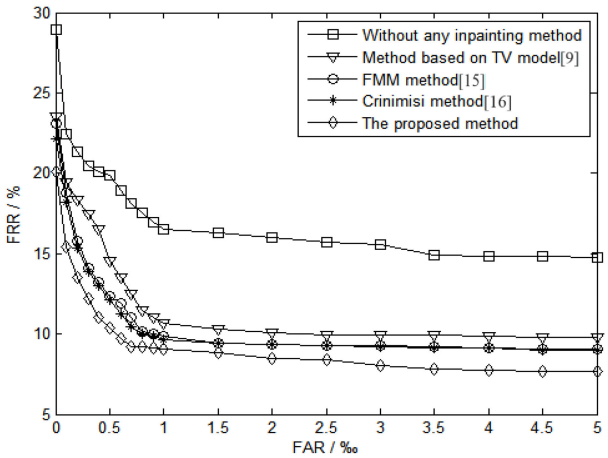

FIGURE 14. Recognition performance of MFVI with images of polluted equipment mirror, after being inpainted by different methods.

The analysis of the above experiments demonstrate that both for the artificially synthetic damaged images and two kinds of acquired damaged images, the proposed method performs better compared with the other three traditional methods. Due to using the Gabor texture constraining mechanism during the inpainting process, the vein texture edge of the images inpainted by the proposed method is more continuous. As a result, the vein skeleton features are more accurate and the recognition performance is also better than three traditional methods without accurate texture constraints.

V. CONCLUSION

This paper proposes a finger vein image inpainting method with Gabor texture constraints, which makes full use of texture information to constrain texture propagation during the inpainting process. The Gabor texture constraining mechanism ensures that the proposed method has a more precise texture propagation so that the vein texture continuity of the inpainted image is better. The proposed method effectively overcomes the problems that the traditional inpainting methods, without accurate texture constraints, easily cause the vein texture edge of the inpainted finger vein images to be blurred and break. Simulation experiments of artificially synthetic images and acquired images demonstrate that the images inpainted by the proposed method have better texture edge continuity and higher quality than traditional image inpainting methods. The proposed method improves the recognition performance of the finger vein identification system for damaged images.

ACKNOWLEDGMENT

The authors would particularly like to thank the anonymous reviewers for their valuable suggestions.

REFERENCES

[1] M. Kono, H. Ueki, and S. Umemura, "A new method for the identification of individuals by using vein pattern matching of finger," in *Proc. Sumposium Pattern Meas.*, Yamaguchi, Japan, 2000, pp. 9–12.

[2] J. Yang, Y. Shi, and J. Yang, "Personal identification based on finger-vein features," *Comput. Hum. Behav.*, vol. 28, pp. 1565–1570, Sep. 2011.

[3] L. Yang, G. Yang, Y. Yin, and R. Xiao, "Finger vein image quality evaluation using support vector machines," *Opt. Eng.*, vol. 52, no. 2, Feb. 2013, Art. no. 027003.

[4] W. You, W. Zhou, J. Huang, F. Yang, Y. Liu, and Z. Chen, "A bilayer image restoration for finger vein recognition," *Neurocomputing*, vol. 348, pp. 54–65, Jul. 2019.
[5] J. Yang and Y. Shi, "Towards finger-vein image restoration and enhancement for finger-vein recognition," *Inf. Sci.*, vol. 268, pp. 33–52, Jun. 2014.
[6] J. Yang and J. Yang, "Multi-channel Gabor filter design for finger-vein image enhancement," in *Proc. 5th Int. Conf. Image Graph.*, Xi'an, Shanxi, Sep. 2009, pp. 87–91.
[7] P. M. Patil and B. H. Deokate, "Image mapping and object removal in image inpainting using wavelet transform," in *Proc. Int. Conf. Inf. Process. (ICIP)*, Pune, India, Dec. 2015, pp. 114–118.
[8] H. Li, W. Luo, and J. Huang, "Localization of diffusion-based inpainting in digital images," *IEEE Trans. Inf. Forensics Security*, vol. 12, no. 12, pp. 3050–3064, Dec. 2017.
[9] T. F. Chan, S. H. Kang, and J. Shen, "Total variation denoising and enhancement of color images based on the CB and HSV color models," *J. Vis. Commun. Image Represent.*, vol. 12, no. 4, pp. 422–435, Dec. 2001.
[10] C. Ballester, M. Bertalmio, V. Caselles, G. Sapiro, and J. Verdera, "Filling-in by joint interpolation of vector fields and gray levels," *IEEE Trans. Image Process.*, vol. 10, no. 8, pp. 1200–1211, Aug. 2001.
[11] T. F. Chan and J. Shen, "Nontexture inpainting by curvature-driven diffusions," *J. Vis. Commun. Image Represent.*, vol. 12, no. 4, pp. 436–449, Dec. 2001.
[12] M. Bertalmio, "Image inpainting," *Siggraph*, vol. 4, no. 9, pp. 417–424, 2005.
[13] J. Dahl, P. C. Hansen, S. H. Jensen, and T. L. Jensen, "Algorithms and software for total variation image reconstruction via first-order methods," *Numer. Algorithms*, vol. 53, no. 1, pp. 67–92, Jan. 2010.
[14] W. Zuo and Z. Lin, "A generalized accelerated proximal gradient approach for total-variation-based image restoration," *IEEE Trans. Image Process.*, vol. 20, no. 10, pp. 2748–2759, Oct. 2011.
[15] A. Telea, "An image inpainting technique based on the fast marching method," *J. Graph. Tools*, vol. 9, no. 1, pp. 23–34, Jan. 2004.
[16] A. Criminisi, P. Perez, and K. Toyama, "Region filling and object removal by exemplar-based image inpainting," *IEEE Trans. Image Process.*, vol. 13, no. 9, pp. 1200–1212, Sep. 2004.
[17] S. Z. Siadati, F. Yaghmaee, and P. Mahdavi, "A new exemplar-based image inpainting algorithm using image structure tensors," in *Proc. 24th Iranian Conf. Electr. Eng. (ICEE)*, Shiraz, Iran, May 2016, pp. 995–1001.
[18] D. J. Tuptewar and A. Pinjarkar, "Robust exemplar based image and video inpainting for object removal and region filling," in *Proc. Int. Conf. Intell. Comput. Control (IC)*, Coimbatore, India, Jun. 2017, pp. 1–4.
[19] A. Bugeau and M. Bertalmio, "Combining texture synthesis and diffusion for image inpainting," in *Proc. Int. Conf. Comput. Vis. Theory Appl.*, 2009, pp. 26–33.
[20] M. Bertalmio, L. Vese, G. Sapiro, and S. Osher, "Simultaneous structure and texture image inpainting," *IEEE Trans. Image Process.*, vol. 12, no. 8, pp. 882–889, Aug. 2003.
[21] C. Qin, S. Wang, and X. Zhang, "Simultaneous inpainting for image structure and texture using anisotropic heat transfer model," *Multimedia Tools Appl.*, vol. 56, no. 3, pp. 469–483, Feb. 2012.
[22] H. Qin and M. A. El-Yacoubi, "Deep representation-based feature extraction and recovering for finger-vein verification," *IEEE Trans. Inf. Forensics Security*, vol. 12, no. 8, pp. 1816–1829, Aug. 2017.
[23] L. Lei, F. Xi, and S. Chen, "Finger-vein image enhancement based on pulse coupled neural network," *IEEE Access*, vol. 7, pp. 57226–57237, 2019.
[24] W. Liu, W. Li, L. Sun, L. Zhang, and P. Chen, "Finger vein recognition based on deep learning," in *Proc. 12th IEEE Conf. Ind. Electron. Appl. (ICIEA)*, Siem Reap, Cambodia, Jun. 2017, pp. 205–210.
[25] Y. Zhang, W. Li, L. Zhang, X. Ning, L. Sun, and Y. Lu, "Adaptive learning Gabor filter for finger-vein recognition," *IEEE Access*, vol. 7, pp. 159821–159830, 2019.
[26] Y. Lu, S. Yoon, S. J. Xie, J. Yang, Z. Wang, and D. S. Park, "Finger vein recognition using histogram of competitive Gabor responses," in *Proc. 22nd Int. Conf. Pattern Recognit.*, Stockholm, Sweden, Aug. 2014, pp. 1758–1763.
[27] J. Wu, P. Wei, X. Yuan, Z. Shu, Y.-Y. Chiang, Z. Fu, and M. Deng, "A new Gabor filter-based method for automatic recognition of hatched residential areas," *IEEE Access*, vol. 7, pp. 40649–40662, 2019.
[28] J. A. Sethian, "Fast-marching level-set methods for three-dimensional photolithography development," in *Proc. 15th Opt. Microlithography*, vol. 2726, Jun. 1996, pp. 262–272.
[29] T. Junwei, H. Yongxuan, and T. Junwei, "Histogram constraint based fast FCM cluster image segmentation," in *Proc. IEEE Int. Symp. Ind. Electron.*, Vigo, Spain, Jun. 2007, pp. 1623–1627.
[30] S. Juan Xie, J. Yang, S. Yoon, L. Yu, and D. S. Park, "Guided Gabor filter for finger vein pattern extraction," in *Proc. 8th Int. Conf. Signal Image Technol. Internet Based Syst.*, Naples, Italy, Nov. 2012, pp. 118–123.
[31] X. M. Guo, W. D. Zhou, and C. Y. Wang, "The segmentation algorithm for hand vein images based on improved Niback algorithm," *Adv. Mater. Res.*, vols. 532–533, pp. 1558–1562, Jun. 2012.
[32] M. Sudarma and N. Putu Sutramiani, "The thinning Zhang–Suen application method in the image of balinese scripts on the papyrus," *Int. J. Comput. Appl.*, vol. 91, no. 1, pp. 9–13, 2014.
[33] M.-P. Dubuisson and A. K. Jain, "A modified Hausdorff distance for object matching," in *Proc. 12th Int. Conf. Pattern Recognit.*, Jerusalem, Israel, vol. 1, 1994, pp. 566–568.
[34] A. Kumar and Y. Zhou, "Human identification using finger images," *IEEE Trans. Image Process.*, vol. 21, no. 4, pp. 2228–2244, Apr. 2012.

HANG YANG is currently pursuing the master's degree with the School of Communication Engineering, Hangzhou Dianzi University. His research interests include biometric recognition and image processing.

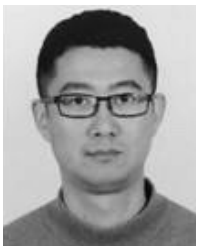

LEI SHEN received the B.Eng. and Ph.D. degrees in electronic engineering from Zhejiang University, Hangzhou, China, in 2002 and 2007, respectively. From 2014 to 2015, he was a Visiting Scholar with the Department of Electrical and Computer Engineering, Stevens Institute of Technology, Hoboken, NJ, USA. He is currently a Professor with the College of Communication Engineering, Hangzhou Dianzi University, Hangzhou. His research interests include vein image processing and signal processing.

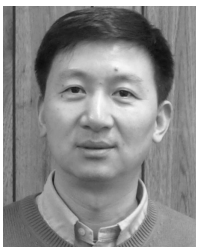

YU-DONG YAO (Fellow, IEEE) received the B.Eng. and M.Eng. degrees in electrical engineering from the Nanjing University of Posts and Telecommunications, Nanjing, China, in 1982 and 1985, respectively, and the Ph.D. degree in electrical engineering from Southeast University, Nanjing, in 1988. From 1987 to 1988, he was a Visiting Student with Carleton University, Ottawa, ON, Canada. From 1989 to 2000, he was with Carleton University, Spar Aerospace Ltd., Montreal, QC, Canada, and Qualcomm Inc., San Diego, CA, USA. Since 2000, he has been with the Stevens Institute of Technology, Hoboken, NJ, USA, where he is currently a Professor and the Chair of the Department of Electrical and Computer Engineering. He holds one Chinese patent and over 13 U.S. patents. His research interests include wireless communications, cognitive radio, machine learning, and deep learning techniques. He served as an Associate Editor for the IEEE COMMUNICATIONS LETTERS, from 2000 to 2008, and the IEEE TRANSACTIONS ON VEHICULAR TECHNOLOGY, from 2001 to 2006. He also served as an Editor for the IEEE TRANSACTIONS ON WIRELESS COMMUNICATIONS, from 2001 to 2005. For his contributions to wireless communications systems, he was elected as the National Academy of Inventors, in 2015, and the Canadian Academy of Engineering, in 2017.

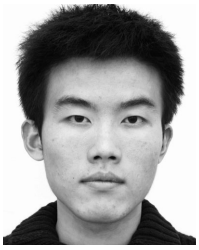

HUAXIA WANG (Member, IEEE) received the B.Eng. degree in information engineering from Southeast University, Nanjing, China, in 2012, and the Ph.D. degree in electric engineering from the Stevens Institute of Technology, Hoboken, NJ, USA, in 2018. From 2016 to 2017, he was a Research Intern with the Mathematics of Networks and Systems Research Department and Nokia Bell Labs, Murray Hill, NJ, USA. He joined Futurewei Technologies Inc., Bridgewater, NJ, USA, in 2018. He is currently a Co-Professor with the Oklahoma State University, Stillwater, OK, USA. He has published more than 15 articles in premium conferences and peer-reviewed journals, including *ICLR*, the IEEE JOURNAL ON SELECTED AREAS IN COMMUNICATIONS, the IEEE TRANSACTIONS ON WIRELESS COMMUNICATIONS, the IEEE TRANSACTIONS ON NEURAL NETWORKS AND LEARNING SYSTEMS, the IEEE TRANSACTIONS ON VEHICULAR TECHNOLOGY, and so on. His research interests include image processing, wireless communications, cognitive radio networks, reinforcement learning, and deep learning. He was a recipient of the Outstanding Ph.D. Dissertation Award in electrical engineering and the Edward Peskin Award with the Stevens Institute of Technology, in 2018.

GUODONG ZHAO received the Ph.D. degree in communication and information system from the Chinese Academy of Sciences, Shanghai, China, in 2008. He is currently a Chief Technology Officer with Top Glory Tech Limited Company, China. His current research interest includes biometric identification technology.